Full Paper Transactions, SMiRT 28
Toronto, Canada, August 10-15, 2025

ASSESSMENT OF INTERNAL PRESSURE FRAGILITY OF CONTAINMENT BUILDING CONSIDERING UNCERTAINTIES IN MATERIAL PROPERTIES AND PRESTRESS LOSS

Gyeonghee An[1] and Tae-Hyun Kwon[2]

[1] Senior Researcher, Korea Atomic Energy Research Institute, Daejeon, Republic of Korea (akh425@kaeri.re.kr)
[2] Principal Researcher, Korea Atomic Energy Research Institute, Daejeon, Republic of Korea (taekwonkr@kaeri.re.kr)

ABSTRACT

The containment building in a nuclear power plant (NPP) serves as the final barrier to prevent the leakage of radioactive materials under severe accident conditions. This study assesses the internal pressure fragility of a prestressed concrete containment building, considering uncertainties in material properties and prestress loss. A 3D finite element model based on APR1400-type NPPs in Korea is used to analyze the nonlinear response of the containment building under internal pressure. Material properties and prestress loss were determined based on literature and site surveys. Two methods, Separation Of Variables (SOV) and Latin Hypercube Sampling (LHS), were used to assess internal pressure fragility, with the failure criteria based on regulatory guidelines. This research determines the failure probability of the containment building under internal pressure. The results can be utilized for Level 2 Probabilistic Safety Assessment (PSA). The results can be utilized for Level 2 Probabilistic Safety Assessment (PSA).

INTRODUCTION

Nuclear power plants (NPPs) incorporate multiple safety barriers to prevent the release of radioactive materials during accidents. Among these barriers, the containment building serves as the final barrier (NEA, 2016), and it must maintain its structural and functional integrity under severe accident conditions. Structural integrity refers to the ability to withstand applied loads without rupture, collapse, or uncontrolled deformation. Functional integrity refers to the ability to maintain its function as a leaktight pressure boundary without significant leakage (RG 1.216, 2010). Ensuring the containment building's integrity under extreme conditions is crucial for maintaining nuclear safety. Following the Great East Japan earthquake in 2011, the need for a robust design of concrete containment structures was highlighted (IAEA, 2011).

Probabilistic safety assessment (PSA) of a NPP provides a comprehensive, structured approach to identifying failure scenarios and deriving numerical estimates of risk. Level 2 PSA identifies how the release of radioactive material from fuel can result in environmental contamination. It also estimates the frequency, magnitude and other relevant characteristics of the release of radioactive material to the environment (IAEA, 2010). The findings of this research can contribute to improving the accuracy of Level 2 PSA by providing a detailed probabilistic assessment of containment building failure.

This study focuses on the internal pressure fragility assessment of a prestressed concrete containment building based on the APR1400-type NPP design in Korea. Internal pressure fragility is defined as the cumulative probability of failure as internal pressure increases. A 3D finite element model is employed to capture the nonlinear response of the structure under pressure loading. Uncertainties in material properties and prestress loss are incorporated based on existing literature and site surveys. Two statistical methods, Separation of Variables (SOV) and Latin Hypercube Sampling (LHS), are utilized to evaluate the fragility of the containment building under internal pressure, with failure criteria aligned with regulatory guidelines.

FINITE ELEMENT MODEL OF CONTAINMENT BUILDING

Geometry of the Containment Building

The containment building investigated in this study is a prestressed concrete structure based on APR1400-type NPPs in Korea. The model includes major penetrations and three buttresses, as shown in Figure 1. The containment wall is 176.5ft(53.8m) tall and 4 ft(1.2m) thick. The dome's diameter is 150ft(45.7m), and the liner plate is 0.25 in.(6 mm) thick. A liner plate is attached to the concrete containment wall, while rebars and tendons are embedded within the concrete.

Figure 1. Finite element model of the containment building

Materials in the Containment Building

The Concrete Damaged Plasticity (CDP) model in ABAQUS is used to represent the concrete material, and the stress-strain relationships are as shown in Figure 2. The parameters for the CDP model are listed in Table 1.

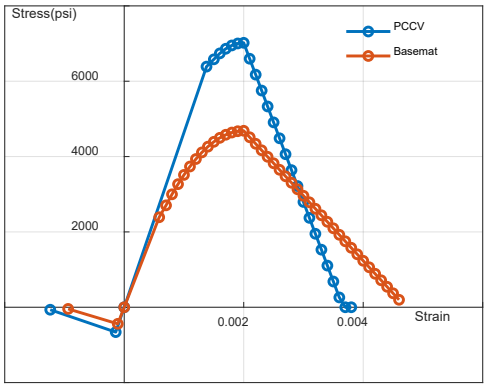

Figure 2. Stress-strain relationship of the basemat and prestressed concrete containment vessel concrete

Table 1: Parameters for the CDP model

Parameters	Values
Dilation angle, ψ	56
Flow potential eccentricity, ϵ	0.1
The ratio of initial equibiaxial compressive yield stress to initial uniaxial compressive yield stress, σ_{b0}/σ_{c0}	1.16
The ratio of the second stress invariant on the tensile meridian to that on the compressive meridian at initial yield, K_c	0.67
Viscosity parameter, μ	0.001

A bilinear model is applied to the steel components, including the liner plate, rebars, and tendons. The stress-strain relationships of the materials are shown in Figure 3.

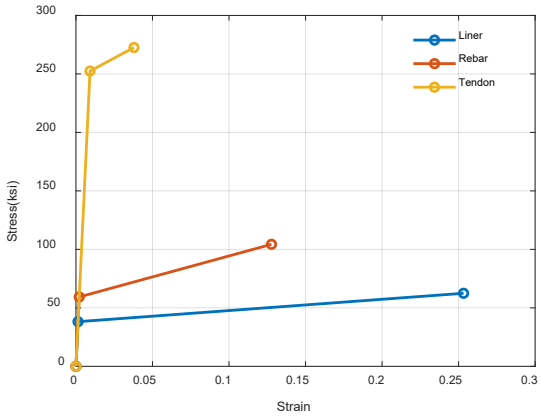

Figure 3. Stress-strain relationship of steel components

Prestress for the Containment Building

According to an industry code in Korea (KEPIC SNB, 2015), the average tensile stress at the anchorage point of a tendon group after anchoring shall not exceed 70% of the ultimate tensile strength of prestressing tendon ($0.70f_{pu}$). This initial prestress decreases due to both instantaneous and long-term factors. If test results related to prestress loss are available, the loss can be calculated following RG 1.35.1(1990). However, in cases where experimental results are unavailable, multiple assumptions must be made. Therefore, in this analysis, the design prestress is conservatively applied, as the actual prestress is assumed to be higher than the design value. The design prestress for an old plant in Korea is as shown in Table 2 (Seo et al. (2000)).

Table 2: Design prestress (Seo et al. (2000))

Type of tendon	Design prestress (ksi)
Vertical tendons	$162.4(0.601f_{pu})$
Horizontal tendons of wall	$163.7(0.606f_{pu})$
Horizontal tendons of dome	$162.8(0.603f_{pu})$

UNCERTAINTIES IN MATERIAL PROPERTIES AND PRESTRESS LOSS

Uncertainties in material properties and prestress loss are considered in the internal pressure analysis.

Uncertainties in Material Properties

Table 3 presents the median strengths and logarithmic standard deviations β of the materials used in this model. The median strengths are referenced from the performance report of the US-APWR containment (Mitsubishi Heavy Industries, Ltd., 2013), which includes material properties similar to those used in APR1400-type NPPs, along with temperature effects. The uncertainties in material properties are determined based on field data acquired from nuclear power plants in Korea. Data from the certified

material test reports (CMTRs) of four plants were analyzed, and the maximum standard deviation for each parameter was conservatively selected, as shown in Table 3.

Table 3: Median strengths and logarithmic standard deviations of materials

Material	Parameter	Median(MPa)	β	95% confidence (MPa)
Basemat Con'c	Compressive strength ($f_{c,base}$)	32.3	0.104	27.2
PCCV Con'c	Compressive strength ($f_{c,\,PCCV}$)	48.4	0.127	39.3
Rebar (A615 Grade 60)	Yield strength (f_y)	409.0	0.071	363.9
	Ultimate strength (f_u)	719.3	0.055	657.0
Liner (SA516 Grade 60	Yield strength (f_y)	263.2	0.037	247.6
	Ultimate strength (f_u)	430.6	0.036	405.8
Tendon (A416 Grade 1860)	Yield strength (f_y)	1740.6	0.015	1698.2
	Ultimate strength (f_u)	1879.4	0.017	1827.5

Uncertainties in Prestress Loss

Uncertainty in prestress loss is determined based on a literature review. Hahm et al. (2010) suggested a logarithmic standard deviation(β) of 0.025, based on measurements from a prestressed test beam of Wolsung Unit 1. Gilbertson and Ahlborn (2004) calculated β based on the variability of 17 input parameters affecting prestress loss, such as yield and ultimate strengths of tendons, jacking stress, unit weight and compressive strength of concrete, relative humidity, and other factors. The value of β was found to range from 0.036 to 0.119. In this study, the maximum value (0.119) is applied for a conservative analysis.

NONLINEAR RESPONSE OF THE CONTAINMENT

The nonlinear response of the containment can be determined through analysis. In this chapter, the analytical results are presented when the median properties are applied to the model. Figure 4 illustrates the overall displacement distribution of the containment at different internal pressure levels (3 and 4 times the design pressure, P_d = 60 psi). The maximum displacement is located near the equipment hatch. According to Figure 4(b), the maximum displacement is approximately 12 inches.

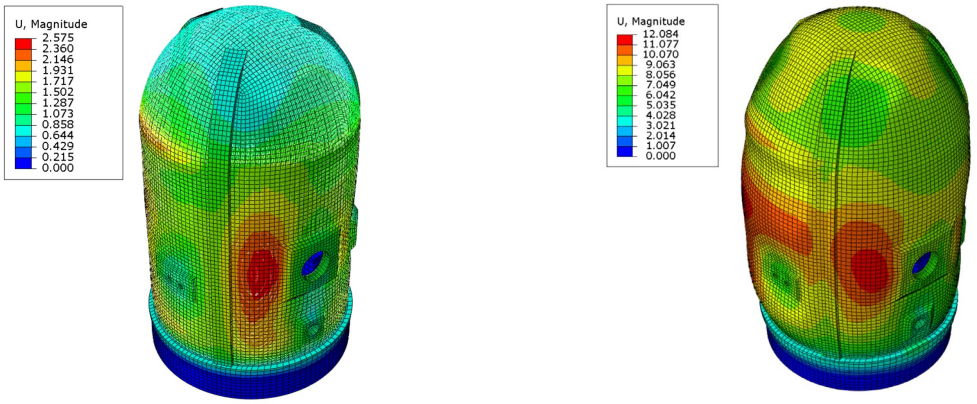

(a) $3P_d$ (b) $4P_d$

Figure 4. Displacement distribution of the containment under internal pressure

The strain distribution of the liner at different internal pressure levels is shown in Figure 5. Similar to displacement results, the maximum strain occurs near the equipment hatch. When the internal pressure reaches $3P_d$, the maximum strain near the hatch exceeds 0.4%, while the free-field strain (away from the discontinuities) remains below 0.4%. However, as the pressure increases, the strain in almost the entire containment wall exceeds 0.4%.

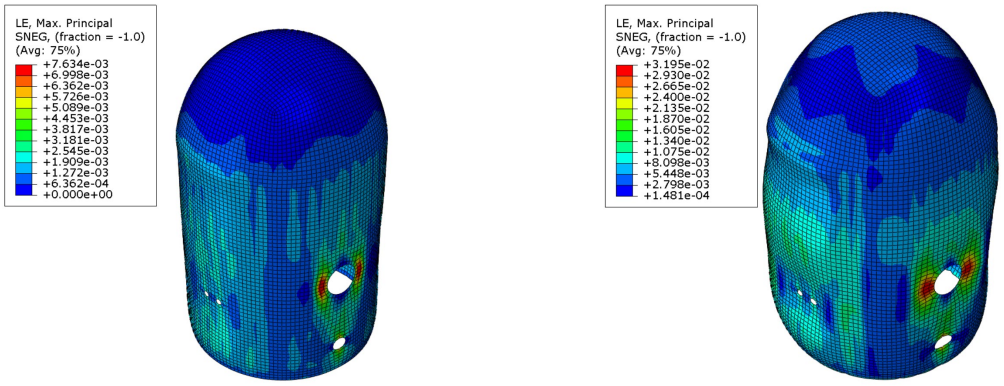

(a) $3P_d$ (b) $4P_d$

Figure 5. Maximum principal strain distribution of the liner plate under internal pressure

The strain distribution of tendons at different internal pressure levels is presented in Figure 6. Again, the maximum strain occurs near the equipment hatch. When the internal pressure reaches $3P_d$, the maximum tendon strain is below 0.8%. However, as the pressure increases, the strain in most of the containment wall exceeds 0.8%.

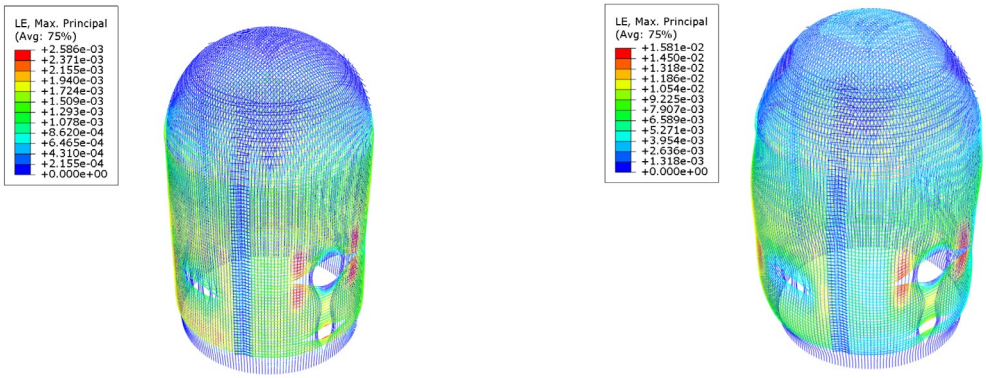

(a) $3P_d$ (b) $4P_d$

Figure 6. Maximum principal strain distribution of tendon under internal pressure

ASSESSMENT OF INTERNAL PRESSURE FRAGILITY

Failure Criteria

RG 1.216 (2010) provides a simplified method for determining the pressure capacity of cylindrical prestressed concrete containment building. The pressure capacity is estimated based on the following strain limits: (1) a total tensile average strain in tendons away from discontinuities (e.g., hoop tendons in a cylinder) of 0.8 percent, and (2) a global free-field strain for the other materials that contribute to resist the internal

pressure (i.e., liner, if considered, and rebars) of 0.4 percent. In this study, these strain limits were applied to determine the pressure capacity, with a point at a height of 212 ft in the containment—away from discontinuities—considered a free-field location.

Separation of Variable Method

The separation of variable method used in this research to develop the fragility is summarized as follows (Mitsubishi Heavy Industries, Ltd., 2013).

1. Determine the median pressure capacity (P_m) using median values of all material properties and prestress condition.
2. An additional analysis with the 95% confidence values of one parameter while keeping all other parameters at their median values. The logarithmic standard deviation for the pressure capacity due to variation in these parameters is then calculated as,
$$\beta_s^i = \frac{\ln(P_s^i/P_m)}{-1.645} \quad (1)$$
where P_s^i is the pressure capacity when evaluated using the 95% confidence value for the i[th] parameter.
3. Assign a logarithmic standard deviation for the pressure capacity due to modeling uncertainties (β_m). This variance for uncertainty is developed using comparisons of analytical predictions to test data results using similar modeling techniques from past work (Mitsubishi Heavy Industries, Ltd., 2013).
4. Calculate a composite lognormal standard deviation for the pressure capacity as the square root of the sum of the squares of all individual standard deviations, as
$$\beta = \sqrt{\Sigma(\beta_s^i)^2 + (\beta_m)^2} \quad (2)$$

The strain of each structural member is determined through analysis, as shown in the previous section. Figure 7 presents the principal strain of the liner plate and tendon at a free-field location as internal pressure increases. The median in the legend represents the analytical result when all median material properties and design prestress are applied. The other cases show analysis results using the 95% confidence values of one property, while keeping all other properties at their median values.

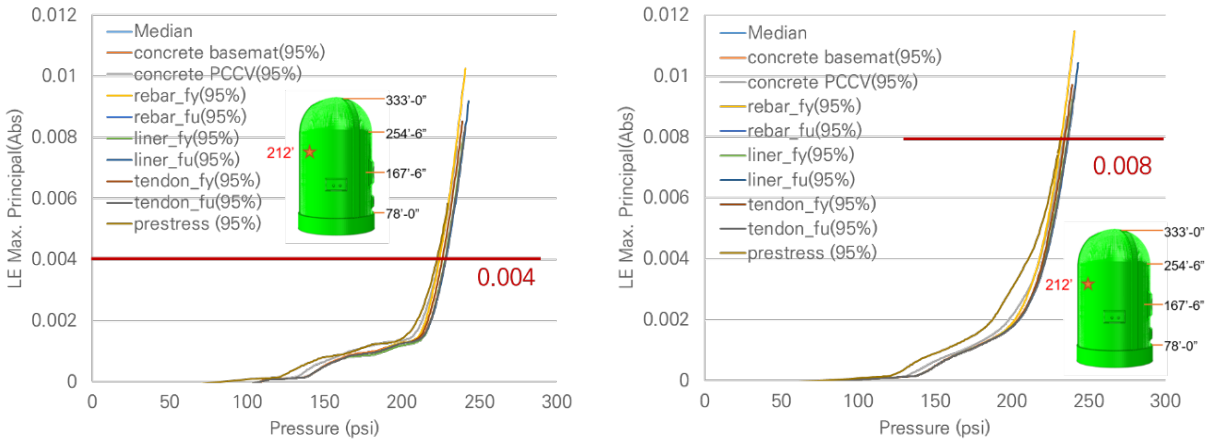

(a) Liner plate (b) Tendon

Figure 7. Global free-field strain with internal pressure

The analysis results are used to determine the internal pressure capacity based on the failure criteria. The internal pressure capacities, based on the strain limits of liner plate and tendons in RG 1.216 (2010), are shown in Table 4. The logarithmic standard deviations for the pressure capacity due to variations in the parameters, β_s^i, are also included in the table. For both criteria, prestress loss, the compressive strength of PCCV concrete, and the yield strength of rebars are the most influential parameters affecting internal pressure capacity.

Table 4: Internal pressure capacity based on the failure criteria in RG 1.216

	Failure criterion: strain of liner plate		Failure criterion: strain of tendon	
	Capacity, P_s^i (psi)	β_s^i	Capacity, P_s^i (psi)	β_s^i
Median	228.21	-	236.82	-
Basemat Con'c (95%)	227.96	0.0007	236.82	0
PCCV Con'c (95%)	223.83	0.0118	233.73	0.0080
rebar_fy (95%)	224.08	0.0111	232.22	0.0119
rebar_fu (95%)	228.08	0.0003	236.67	0.0004
liner_fy (95%)	227.70	0.0014	236.12	0.0018
liner_fu (95%)	228.21	0.0000	236.77	0.0001
tendon_fy (95%)	225.89	0.0062	234.56	0.0058
tendon_fu (95%)	228.00	0.0006	236.56	0.0007
Prestress (95%)	222.55	0.0153	231.78	0.0131

Mitsubishi Heavy Industries, Ltd.(2013) suggested $\beta_m = 0.13$, which is adopted for this study. The composite lognormal standard deviations(β), calculated based on the criteria for the liner plate and tendon, are 0.1320 and 0.1316, respectively.

Latin Hypercube Sampling Method

The Latin Hypercube Sampling(LHS) method was also used in this research, along with the SOV method, to develop the internal pressure fragility. A set of 30 samples, based on the material properties in Table 3 and the prestress loss described in the previous subsection, was generated and used as input for analysis.

At various internal pressure levels, the failure probability was calculated by counting the number of samples where the free-field strain of the liner or tendon exceeded the failure criteria. The blue dots in Figure 8 represent the failure probability of the liner plate and tendon.

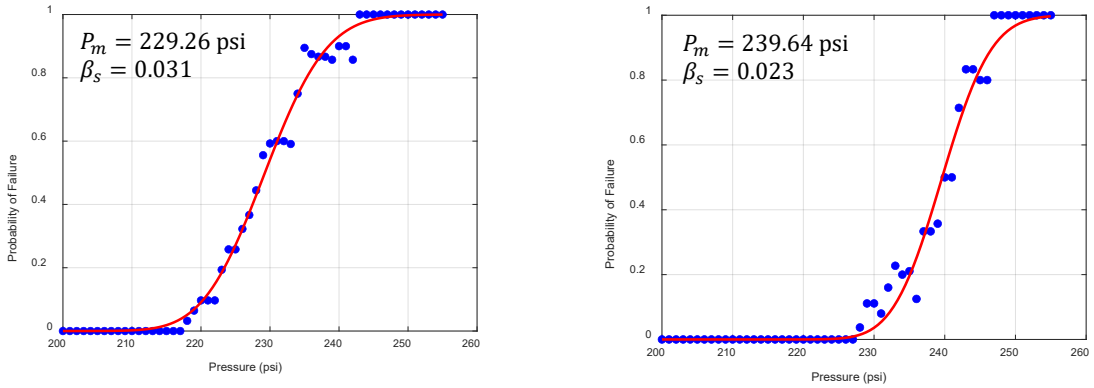

(a) Failure of liner plate (b) Failure of tendon

Figure 8. Probability of failure obtained using LHS method

A lognormal cumulative distribution function is used to define a fragility function, P_f, as follows:

$$P_f = \Phi\left[\frac{\ln(P/P_m)}{\beta_s}\right] \tag{3}$$

where $\Phi[\cdot]$ is the standard normal cumulative distribution function, P_m is the median pressure, and β_s is the logarithmic standard deviation.

The median pressure and logarithmic standard deviation for the pressure capacity, accounting for uncertainties in material properties and prestress loss, are determined as shown in Figure 8 using a curve-fitting function in MATLAB.

Modeling uncertainties could not be considered in the LHS; therefore, the logarithmic standard deviation due to modeling uncertainties(β_m) is assumed to be the same as that in the SOV method. The composite lognormal standard deviations(β), calculated from β_s and β_m based on the criteria for the liner plate and tendon, are 0.1336 and 0.132, respectively.

Internal Pressure Fragility

The internal pressure fragility curves obtained from the SOV and LHS methods are shown in Figure 9. The choice of fragility assessment method did not significantly affect the fragility of the containment, as shown in Figure 9. The median pressure, composite logarithmic standard deviation and High-Confidence Low-Probability of Failure (HCLPF) values for internal pressure fragility are presented in Table 5.

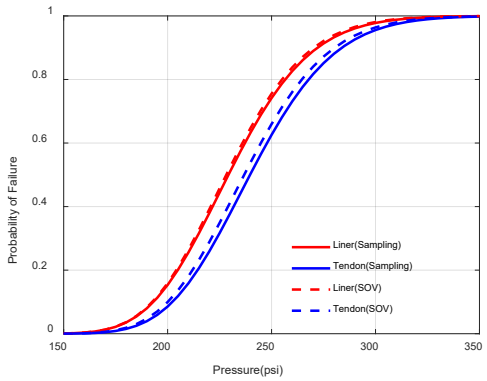

Figure 9. Internal pressure fragility curves from SOV and LHS methods

Table 5: Median pressure, composite logarithmic standard deviation and HCLPF values for internal pressure fragility

	Failure criterion: strain of liner plate		Failure criterion: strain of tendon	
	SOV	LHS	SOV	LHS
P_m (psi)	228.21	229.26	236.82	239.64
β	0.1320	0.1336	0.1316	0.1320
HCLPF(psi)	167.87	168.016	174.365	176.28

CONCLUSION

This study investigated the nonlinear response and internal pressure fragility of a prestressed concrete containment building based on the APR1400-type nuclear power plant.

The maximum displacement and strain occur near the equipment hatch, with the free-field regions experiencing lower strains. The internal pressure capacity was assessed based on failure criteria specified in RG 1.216 (2010), considering strain limits for the liner plate and tendons at the free-field location.

Two methods, the SOV and LHS, were used to evaluate the containment's internal pressure fragility. The SOV method revealed that prestress, concrete compressive strength, and rebar yield strength are the most influential factors for the containment capacity. The choice of fragility assessment method did not significantly affect the fragility of the containment. Based on the liner failure criterion, the median pressure and HCLPF value for this containment were calculated approximately $3.8P_d$ and $2.8P_d$, respectively.

The findings in this research can contribute to improved safety assessments and risk evaluations for nuclear power plant containment structures. Future studies could incorporate additional factors such as aging effects, suggestion of the failure criteria, and experimental validation to enhance the accuracy of fragility assessments.

ACKNOWLEDGEMENTS

This work was supported by the National Research Foundation of Korea (NRF, No. RS-2022-00144409) and the Korea Institute of Energy Technology Evaluation and Planning (KETEP, 20224B10300010).

REFERENCES

Gilbertson, C. and Ahlborn, T. (2004) "A Probabilistic Comparison of Prestress Loss Methods in Prestressed Concrete Beams", PCI Journal, Vol. 49, No. 5, pp.52-69.

Hahm, D., Choi, I. and Lee, H. (2010) "Assessment of Internal Pressure Fragility of the CANDU Type Containment Buildings using Nonlinear Finite Element Analysis", *Journal of the Computational Structural Engineering Institute of Korea*, Vol. 23, No. 4, pp.445-452.

IAEA (2010) Development and Application of Level 2 Probabilistic Safety Assessment for Nuclear Power Plants, IAEA Safety Standards Series No. SSG-4, IAEA, Vienna

IAEA (2011) International fact finding expert mission of the Fukushima Dai-ichi NPP accident following the Great East Japan earthquake and tsunami. Tokyo, Fukushima Dai-ichi NPP, Fukushima Dai-ni NPP and Tokai Dai-ni NPP, Japan.

Korea Electric Power Industry Code(KEPIC) SNB (2015) *Concrete Containments*, Korea Electric Association.

Mitsubishi Heavy Industries, Ltd. (2013) "US-APWR Containment Performance for Pressure Load", Tokyo, *MUAP-10018-NP(R1)*

NEA (2016), Implementation of Defence in Depth at Nuclear Power Plants, OECD Publishing, Paris

Regulatory guide 1.216. (2010) *Containment structural integrity evaluation for internal pressure loading above design-basis pressure*, U.S. Nuclear Regulatory Commission, Washington, D.C.

Regulatory guide 1.35.1(Task SC 807-4) (1990) *Determining prestressing forces for inspection of prestressed concrete containments*, U.S. Nuclear Regulatory Commission, Washington, D.C.

Seo, J., Choi, I. and Bae, I. (2000) "Analysis of in-service inspection guides for prestress concrete containment buildings", KAERI, Daejeon, *KAERI/TR-1504/2000.*